

# Optimal Catalyst Activity Profiles in Pellets: 9. Study of Ethylene Epoxidation

Asterios Gavrilidis and Arvind Varma

Dept. of Chemical Engineering, University of Notre Dame, Notre Dame, IN 46556

*The concept of optimal catalyst activity distribution is studied experimentally for the ethylene epoxidation reaction network on a  $\text{Ag}/\alpha\text{-Al}_2\text{O}_3$  catalyst in a single-pellet reactor. The Dirac delta-type distribution of the catalyst is approximated by a step distribution of narrow width. For a fixed amount of silver, the influence of location and width of the catalytically active layer on the conversion of ethylene and on the selectivity and yield to ethylene oxide is investigated under oxygen-rich conditions in the temperature range 210–270°C. The results clearly demonstrate that for optimum selectivity and yield to ethylene oxide, the silver catalyst should be placed in a thin layer at the external surface of the pellet.*

## Introduction

The effects of nonuniform distribution of the catalytic material within the support in the performance of a catalyst pellet started receiving attention in the late 60s (cf. Michalko, 1966; Kasaoka and Sakata, 1968; Minhas and Carberry, 1969; Roth and Reichard, 1972; Shadman-Yazdi and Petersen, 1972). These, as well as later studies, both theoretical and experimental, demonstrated that nonuniformly distributed catalysts can offer superior conversion, selectivity, durability, and thermal sensitivity characteristics over those in which the activity is uniform. Work up to 1987 has been reviewed (Dougherty and Verykios, 1987).

For a fixed total amount of catalyst, Morbidelli et al. (1982) examined the issue of its optimal distribution for the case of a reaction following bimolecular Langmuir-Hinshelwood kinetics, occurring in an isothermal pellet with negligible external mass transfer resistance. They showed analytically that among any *arbitrary* catalyst distribution, the optimal one is an appropriately chosen Dirac-delta function. It was also shown that a Dirac-delta distribution could be approximated in practice with a step distribution of the catalyst, if the width of the active zone was kept less than about 5% of the characteristic particle dimension. This theory was later extended to include the influence of external mass transfer resistance (Morbidelli and Varma, 1982), nonisothermal pellets (Morbidelli et al., 1985), arbitrary reaction kinetics (Chemburkar et al., 1987; Vayenas and Pavlou, 1987), and complex reaction networks (cf. Vayenas and Pavlou, 1988). Recently, Wu et al. (1990a)

showed that for any catalyst performance index (conversion, selectivity, or yield) and for the most general case of an arbitrary number of reactions, following arbitrary kinetics, occurring in a nonisothermal pellet, with finite external mass and heat transfer resistances, the optimal catalyst distribution remains a Dirac delta function.

As compared with theoretical work, only relatively few experimental studies have been reported. Chemburkar (1987) and Lee and Varma (1988) investigated the performance of  $\text{Pt}/\gamma\text{-Al}_2\text{O}_3$  catalysts in a recycle reactor and in a fixed-bed reactor for CO oxidation, respectively. The catalyst, in which the Pt was deposited as a narrow band in the desired location inside the pellet, was prepared by impregnation techniques. Similar  $\text{Pt}/\gamma\text{-Al}_2\text{O}_3$  catalyst pellets were used by Masi et al. (1988), who studied  $\text{C}_2\text{H}_4$  hydrogenation in a recycle reactor. Wu and coworkers studied CO methanation on  $\text{Ni}/\gamma\text{-Al}_2\text{O}_3$  (1988, 1990b) and  $\text{C}_2\text{H}_4$  hydrogenation on  $\text{Pd}/\gamma\text{-Al}_2\text{O}_3$  (1988). They used a single-pellet Berty reactor, for which step-type catalyst pellets were prepared mechanically.

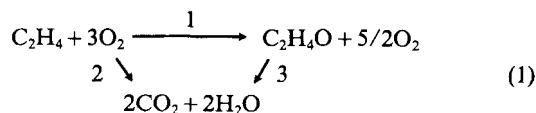
The ethylene epoxidation reaction network, occurring in a Dirac type catalyst, has previously been studied theoretically (Morbidelli et al., 1984; Pavlou and Vayenas, 1990). Both studies showed that the selectivity to ethylene oxide is maximized when the catalyst is located at the surface of the pellet for an egg-shell-type catalyst. Morbidelli et al. (1984) also showed that the amount of ethylene oxide produced could be maximized using catalysts where the active material is located in the interior of the pellet at a position that depends on the physicochemical parameters of the system. However, no ex-

Correspondence concerning this article should be addressed to A. Varma.

perimental investigation of the performance of such catalysts for this industrially important reaction network has been reported. The present work describes results of such an experimental study.

## Experimental Study

Ethylene reacts over supported silver catalyst with oxygen to give ethylene oxide. Important side reaction is the complete combustion of ethylene and to a lesser extent that of ethylene oxide, according to the scheme:



Although this reaction network has been studied extensively, its mechanism is still under debate (Van Santen and Kuipers, 1987). In this study, a single-pellet reactor was used, and the pellet was prepared mechanically by pressing the active catalyst layer between two alumina layers. In this way, a step-type catalyst pellet was produced, which approximated a Dirac-type catalyst distribution.

### Catalyst pellet

The silver catalyst was prepared by impregnation of – 325 mesh  $\alpha$ -alumina powder, using a procedure similar to that of Klugherz and Harriott (1971). The  $\alpha$  alumina used was Alcoa A-17 with a surface area of 3 m<sup>2</sup>/g; 15 mL of lactic acid (85%, Fisher Scientific) was heated to 90°C; and 5.2 g of silver oxide (Fisher Scientific) and 0.4 mL of hydrogen peroxide (15%, Aldrich) were then added to the continuously stirred solution. After the silver oxide dissolved completely, 10 g of  $\alpha$ -alumina powder was added. The excess solution was evaporated, and then the particles were dried at 220°C in air for 24 hours. To decompose the silver lactate, the catalyst was heated at 500°C under nitrogen for 5 hours. After cooling, it was subjected to two oxidation reduction cycles at 350°C. This treatment was necessary to get a catalyst with stable activity, and one cycle consisted of oxidizing the active powder with a mixture of 20% oxygen in argon for three hours, flushing the system with nitrogen for 10 min, reducing it with a mixture of 20% hydrogen in argon for three hours, and flushing it again with nitrogen for 10 min. At the end of the second cycle, the catalyst was cooled in nitrogen. In this way, the *active powder* was obtained, which contained 33.8 wt. % silver. The loading was also confirmed by atomic absorption spectroscopy.

The silver surface area was determined by selective chemisorption of oxygen in a pulse chemisorption apparatus at 200°C. At this temperature, oxygen monolayer coverage of silver occurs, and the stoichiometry of chemisorption corresponds nearly to one oxygen atom per surface silver atom (Czanderna, 1964). A site density of  $1.15 \cdot 10^{15} \text{ Ag}_s \cdot \text{cm}^{-2}$  (Satterfield, 1980) was used to calculate the silver surface area, which was 1,340 cm<sup>2</sup>/g catalyst. Assuming that the silver particles were hemispherical in shape, the average crystallite size was calculated to be 680 nm.

Blank runs conducted with pellets made from  $\alpha$  alumina alone showed that it was somewhat reactive toward ethylene oxide combustion and isomerization to acetaldehyde. To minimize this activity, the  $\alpha$ -alumina was impregnated with sodium

hydroxide following the procedure of Lee et al. (1988): 0.3 g of sodium hydroxide (Fisher Scientific) was dissolved in 80-mL distilled water; 100-g  $\alpha$ -alumina powder was added and the excess solution was evaporated at 90°C, while stirring. The particles were dried in air at 150°C for 2 hours and then calcined in air at 500°C for 18 hours. This sodium impregnated  $\alpha$ -alumina support is the *inert powder*.

It is worth noting here that other  $\alpha$ -alumina supports were also tried, but they either showed higher combustion/isomerization of the ethylene oxide (United T-375), or the active powder that was produced had low activity toward ethylene epoxidation (Norton 5202).

The catalyst pellet with the step distribution of the active layer was prepared by pressing together two inert powder layers and one active layer in a two-piece die. The three layers were first pressed at 4,000 psi (27 MN/m<sup>2</sup>), and then the pellet was pressed at 7,000 psi (48 MN/m<sup>2</sup>). The pellet was cylindrical, 20.4 mm in diameter and 7.1 mm in thickness. For all pellets, 0.45 g of active powder and 4.55 g of inert powder were used. Two types of pellets were prepared: type 1, in which the active powder was used as such and positioned at different locations  $s$  from the top surface whose thickness of the active layer was 0.45 mm; type 2, in which the active powder was mixed with some inert powder and again pressed in a layer form. All but one set of experiments (cf. Figure 6) were conducted with type 1 pellets. For convenience, pellets with the active layer at the top surface and below the top surface are referred to as *surface* and *subsurface* catalyst pellets, respectively. The curved surface of the pellet was wrapped with flexible Teflon tape and pressed fit into a sample holder made of Teflon. The pellet was thus thermally insulated from the surroundings, and the reaction gases would diffuse in and out of the pellet only through the top surface.

### Apparatus

The gases, oxygen (Linde, zero grade) and ethylene (Linde, CP grade), were passed through gas purifiers for removing any trace of water. To ensure that no particles escaped the gas purifiers, gas filters with openings of 7  $\mu\text{m}$  were used. The gas flow rates were controlled using Unit UFC-1000 mass flow controllers, interfaced with a Unit URS-5-100 power supply. The gases were then mixed and delivered to the reaction section.

The reaction unit consisted of a preheater that was used not only to preheat the reaction gases, but also to promote mixing of the recycle stream with the fresh feed. The gases were then delivered to the reactor that was heated by two semicylindrical heating elements. A small portion of the gas exiting the reactor was delivered to the analysis section, while the majority was recycled using a diaphragm pump. The recycle ratio was about 170, so CSTR conditions (a well-mixed fluid phase) were ensured.

The reactor was a specially designed *single-pellet reactor*, shown in Figure 1. It consisted of two stainless steel tubes of rectangular cross-section. The dimensions of the outer tube were 75 cm long, 4.45 cm wide and 4.45 cm high, while those of the inner tube were 75 cm long, 3.86 cm wide, and 3.23 cm high. The tubes were constructed such that one fit tightly into the other, leaving a channel of rectangular cross-section, through which the reaction gases passed. The sample holder which contained the catalyst pellet was placed in such a way that its top surface was flush with the reaction gases flowing

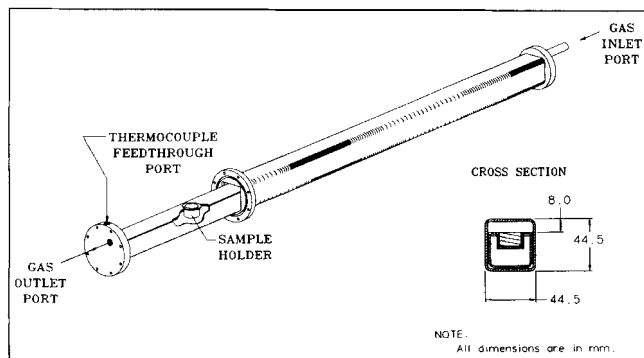


Figure 1. Single-pellet reactor.

parallel to its top surface. The length of the tube upstream of the pellet was sufficient for the flow to develop fully. The flange at one end of the reactor had a feedthrough that was used to insert a thermocouple that recorded the temperature of the reaction gas just above the pellet.

The gases exiting the reactor passed through a Beckman 565 infrared  $\text{CO}_2$  analyzer, which continuously monitored the production of carbon dioxide. Gas composition analysis was performed on-line using a Hewlett Packard 5890 II gas chromatograph, equipped with both a thermal conductivity and a flame ionization detector. The injection of the sample to the chromatograph was made by means of a Valco 6-way sampling valve, with one 100- $\mu\text{L}$  sampling loop. The gases were separated by a Porapak-Q 1.8-m-long, 3.2-mm-OD, stainless steel column, packed with 100-120 mesh particles. The column temperature was kept at  $90^\circ\text{C}$ , and ultra-high-purity helium was used as the carrier gas. The data were collected and analyzed using a Hewlett Packard 3396 II integrator. A combination of four-way valves, toggle valves and needle valves allowed the calibration of the infrared  $\text{CO}_2$  analyzer and of the chromatograph, and periodic checking of the feed composition using the gas chromatograph. The lines from the reactor exit to the sampling valve were heated at about  $70^\circ\text{C}$  to prevent condensation of the water that was produced.

### Procedure

After the pellet was loaded into the reactor, it was aged for 24 hours at  $280^\circ\text{C}$  under 2.7 vol. % inlet ethylene concentration and balance oxygen, and then the temperature was decreased to  $210^\circ\text{C}$  where it remained overnight. These conditions (2.7% inlet ethylene concentration, balance oxygen, bulk temperature  $210^\circ\text{C}$ ) will subsequently be referred to as the *standard conditions*. Data were collected for the standard conditions, and then the feed composition was set to the desired value. During a typical day, data were collected for the set feed composition and for five different temperature values between  $210$ – $270^\circ\text{C}$ . At the end of the day, the catalyst was returned to the standard conditions where it remained overnight. This procedure was repeated until the desired composition range (five settings between 1.1–9.9% ethylene, balance oxygen) was covered. The above procedure was necessary to get reproducible results, and it also provided a periodic checking of the activity of the catalyst, which remained essentially constant over the course of the experiment. Five different pellets were used with the distance of the active layer from the top surface ranging be-

tween 0 and 3.19 mm. The total external flow rate was kept fixed at 100 mL/min and the reactor pressure at 15.6 psi (107 kN/m<sup>2</sup>). Under the conditions used for these experiments, no measurable ethylene or ethylene oxide homogeneous or wall reaction was observed. No reaction products other than ethylene oxide, carbon dioxide and water were detected. Carbon balances typically closed to within 2%, and this error never exceeded 6%.

### Definitions

The overall conversion of ethylene,  $X$ , is defined as:

$$X = \frac{[(F_{\text{C}_2\text{H}_4})_{\text{in}} - (F_{\text{C}_2\text{H}_4})_{\text{out}}]}{(F_{\text{C}_2\text{H}_4})_{\text{in}}}, \quad (2)$$

where  $F$  is molar flow rate. The selectivity,  $S$ , to ethylene oxide is defined as:

$$S = \frac{(F_{\text{C}_2\text{H}_4\text{O}})_{\text{out}}}{[(F_{\text{C}_2\text{H}_4})_{\text{in}} - (F_{\text{C}_2\text{H}_4})_{\text{out}}]}, \quad (3)$$

while the yield,  $Y$ , is:

$$Y = XS. \quad (4)$$

The net reaction rates for total ethylene consumption,  $R_{\text{C}_2\text{H}_4}$ , and for ethylene conversion to carbon dioxide,  $R_{\text{CO}_2}$ , and ethylene oxide,  $R_{\text{C}_2\text{H}_4\text{O}}$ , can be calculated from the corresponding mass balances to be:

$$R_{\text{C}_2\text{H}_4} = (F_{\text{C}_2\text{H}_4})_{\text{in}} - (F_{\text{C}_2\text{H}_4})_{\text{out}} \quad (5)$$

$$R_{\text{C}_2\text{H}_4\text{O}} = (F_{\text{C}_2\text{H}_4\text{O}})_{\text{out}} \quad (6)$$

$$R_{\text{CO}_2} = (F_{\text{CO}_2})_{\text{out}}. \quad (7)$$

It is apparent from the definitions above that the yield to ethylene oxide,  $Y$ , is proportional to the net ethylene oxide production  $R_{\text{C}_2\text{H}_4\text{O}}$ , while the conversion of ethylene,  $X$ , is proportional to  $R_{\text{C}_2\text{H}_4}$ .

### Results and Discussion

The catalyst pellets showed stable activity with time. Conversion, selectivity, and yield remained essentially constant over the duration of the experiment, which for each pellet lasted about six days. The maximum deviation in conversion and selectivity from the corresponding average values was 6.5%. Furthermore, by scanning the temperature range several times, in both increasing and decreasing order, it was determined that the reproducibility was very good and that multiple steady states were not present.

The net reaction rates are plotted as a function of the bulk ethylene partial pressure for the surface ( $s = 0$  mm) and one subsurface ( $s = 0.64$  mm) catalyst pellet in Figure 2. There is a monotonic increase of the net ethylene consumption and net carbon dioxide production with temperature. The reaction rates show a saturation behavior for the temperature of  $210^\circ\text{C}$ , but a sharp increase at higher ethylene partial pressures for all the

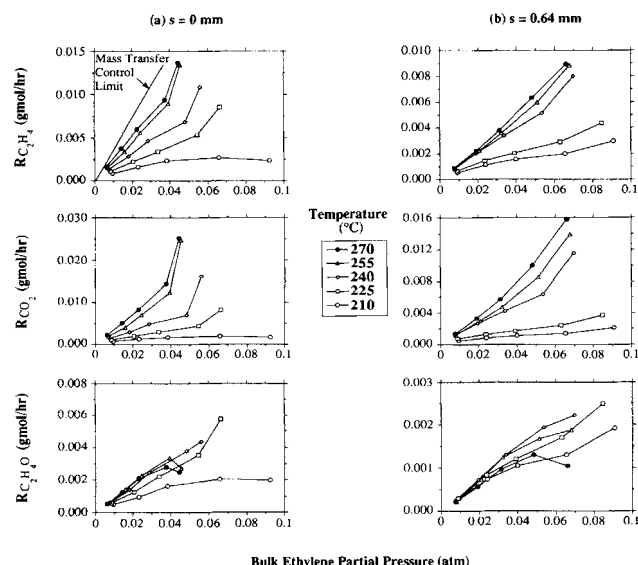


**Figure 2.** Net reaction rates as functions of bulk ethylene partial pressure in reactor for various bulk fluid temperatures: (a)  $s = 0$  mm, (b)  $s = 0.64$  mm.

higher temperatures for  $R_{C_2H_4}$  and  $R_{CO_2}$ ; for  $R_{C_2H_4O}$ , the sharp increase occurs only at 225°C. At higher temperatures, maxima in the curves of  $R_{C_2H_4O}$  are observed. For  $s = 0$  mm (Figure 2a) and a fixed bulk partial pressure of ethylene, the increase in  $R_{CO_2}$  between 255°C and 270°C is higher than the corresponding increase in  $R_{C_2H_4}$ . This, along with the fact that ethylene oxide production begins to decrease when temperature increases beyond 255°C, indicates that combustion of ethylene becomes important above 255°C. The  $R_{C_2H_4}$  curves for the temperatures 255°C and 270°C are close, because the rate approaches the mass transfer control limit, which is also shown in the figure.

Similar behavior is observed for the subsurface catalyst in Figure 2b (note difference in ordinate scales as compared with Figure 2a). In this case, the additional mass transfer resistance introduced by the outer inert layer causes the  $R_{C_2H_4}$  and the  $R_{CO_2}$  curves for 240°C to approach the corresponding ones for 255 and 270°C. Thus, for the subsurface catalyst, the ethylene consumption and carbon dioxide production become diffusion-limited at a lower temperature of 240°C. Also, above this temperature, ethylene oxide production decreases. Although not shown here for brevity, the same trend continues for pellets where the active layer is located deeper inside. Thus, diffusion-limited behavior begins to appear, and ethylene oxide production begins to decrease, at progressively lower temperatures.

Although all the net reaction rate curves for 210°C show a saturation for the surface catalyst (Figure 2a), they continue to rise for the subsurface catalyst (Figure 2b). This can be attributed to the lower ethylene concentration at the location of the active layer for the subsurface catalyst. It may be observed that the net reaction rates are very similar for the surface catalyst ( $s = 0$  mm) and the subsurface catalyst ( $s = 0.64$  mm), when the corresponding bulk ethylene partial pressures are 0.065 atm (6.6 kN/m<sup>2</sup>) and 0.09 atm (9.1 kN/m<sup>2</sup>) respectively.

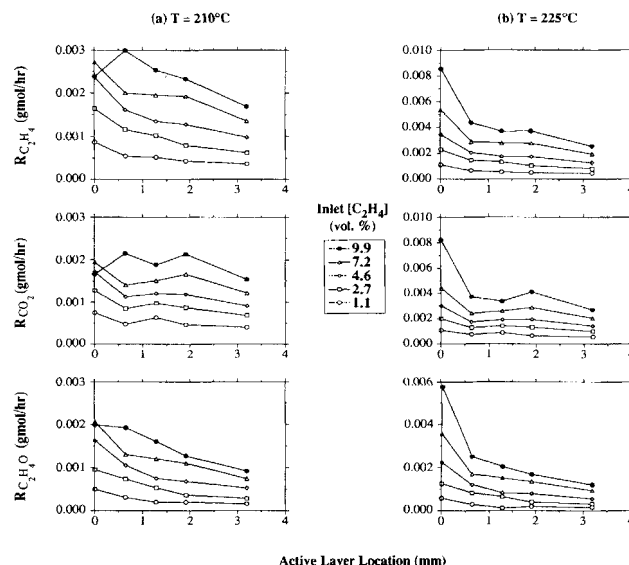


**Figure 3.** Net reaction rates as functions of position of the active layer for various inlet ethylene concentrations: (a)  $T = 210^\circ\text{C}$ , (b)  $T = 225^\circ\text{C}$ .

A “runaway” condition is observed for the surface catalyst when a certain ethylene partial pressure is reached. This critical partial pressure is higher for lower reaction temperatures. Since this type of behavior occurs for the surface catalyst, it indicates the importance of external transfer resistances. For the subsurface catalyst, owing to the presence of intrapellet transport resistances in addition to the external transfer resistances, the runaway condition is not observed so dramatically for the range of ethylene partial pressures investigated.

The dependence of the net reaction rates on the location of the active layer, at 210°C and 225°C, is shown in Figure 3. It is interesting to note that  $R_{C_2H_4}$  and  $R_{CO_2}$  show a maximum for subsurface locations when the temperature is 210°C and the feed contains 9.9% ethylene. This behavior results from intraphase temperature gradients and is qualitatively consistent with previous theoretical findings. It has been shown (Morbidelli et al., 1985; Chemburkar et al., 1987; Vayenas and Pavlou, 1987) that even for positive-order reactions, the optimum location to maximize catalyst effectiveness moves toward the pellet interior, if the product of the dimensionless heat of reaction  $\beta$  and dimensionless activation energy  $\gamma$  is sufficiently large and occurs solely because of the intrapellet temperature gradient. This product is proportional to the reactant concentration, and inversely proportional to the square of the bulk temperature,  $\beta\gamma \sim C_f/T_f^2$ . The highest  $\beta\gamma$  possible in the present work would therefore occur for the lowest temperature (210°C) and for the highest ethylene concentration (9.9% ethylene) studied, where we, in fact, do observe higher  $R_{C_2H_4}$  in the first two subsurface locations and higher  $R_{CO_2}$  in the first three subsurface locations, as compared to the surface values. For lower ethylene concentrations (see Figure 3a) and higher temperatures (compare Figures 3a and 3b), which correspond to smaller  $\beta\gamma$  values, these maxima are no longer observed. This trend is also consistent with the theoretical study of ethylene epoxidation in Dirac-type catalysts (Morbidelli et al., 1984), where it was shown that under the same operating conditions, the effectiveness factor (proportional to  $R_{C_2H_4}$  for

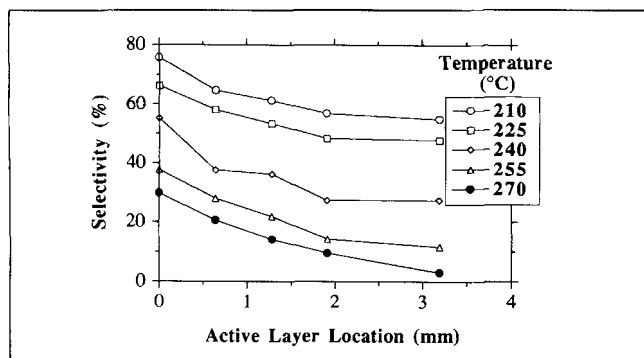


Figure 4. Selectivity as a function of position of the active layer for various bulk fluid temperatures: inlet ethylene concentration = 7.2%.

our case) is maximized at a deeper location than the yield (proportional to  $R_{C_2H_4O}$  for our case). Indeed, by inspecting Figure 3a, it may be seen that  $R_{C_2H_4}$  is maximized at  $s = 0.64$  mm, while  $R_{C_2H_4O}$  is maximized at the next shallower location that was investigated, which was the surface one,  $s = 0$  mm. At this point, it should be emphasized that the numerical values of the maxima in  $R_{C_2H_4}$  and  $R_{CO_2}$  observed for subsurface locations discussed above are much smaller than the values that can be attained at higher temperatures for the surface catalyst. When the temperature is raised to 225°C, all the reaction rates drop significantly when moving from the surface to the first subsurface location (see Figure 3b). The decrease is more significant at higher inlet ethylene concentrations.

As noted earlier, previous theoretical studies (Morbidelli et al., 1984; Pavlou and Vayenas, 1990) have shown that the selectivity to ethylene oxide is maximized, when the active material is located at the surface of the pellet. This behavior results primarily from the fact that the main undesired reaction 2 has a higher activation energy than the desired one. Therefore, intraphase temperature gradients are detrimental to the selectivity. Indeed, in Figure 4, it is shown that at all the temperatures studied, selectivity decreases when the active layer is located deeper inside the pellet. This behavior was observed for all the inlet ethylene concentrations investigated.

A convenient way to summarize the influence of active layer location on catalyst performance is to examine the selectivity

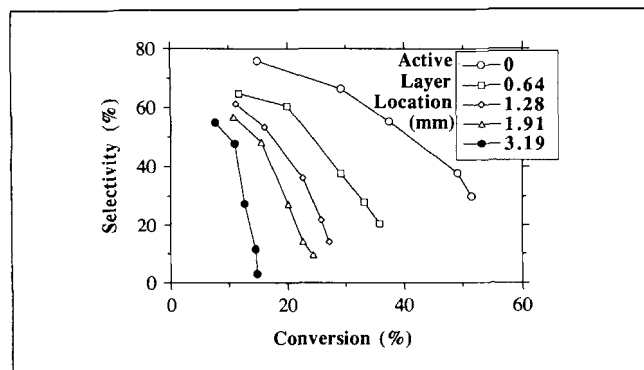


Figure 5. Selectivity as a function of conversion for various active layer locations: inlet ethylene concentration = 7.2%.

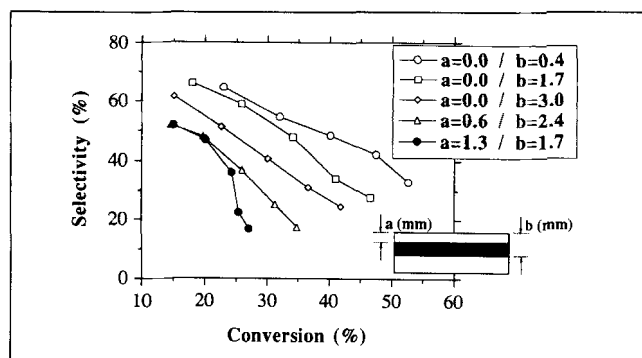


Figure 6. Selectivity as a function of conversion for various active layer locations and widths: inlet ethylene concentration = 2.7%.

vs. conversion behavior. For the five catalyst pellets studied and for the case where the inlet ethylene concentration is 7.2%, this behavior is shown in Figure 5. For each active layer location, the conversion increase was attained by increasing the reaction temperature; this causes the selectivity to decrease, which is typical for the ethylene epoxidation reaction network. This figure shows clearly that selectivity, conversion, and yield are always higher for the surface catalyst pellet. (Note that yield maximization corresponds to operation as close to the upper righthand corner of the graph as possible.) If, for example, an ethylene conversion of 20% is desired, then the surface pellet operated at about 215°C will give ethylene oxide selectivity of about 72%, while the first subsurface pellet ( $s = 0.64$  mm) has to be operated at 225°C and will give a selectivity of only about 60%. When the active layer is placed deeper within the pellet, the reaction has to be carried out at progressively higher temperatures and gives progressively lower selectivities.

A final set of experiments was performed to investigate the effect of the *width* of the active layer, which was changed by mechanically mixing the active powder with the appropriate amount of inert powder before pelletizing (type 2 pellets). In Figure 6, the selectivity vs. conversion behavior for five different pellets with different distances of the active layer from the top surface (denoted in the figure by " $a$ ") and different widths (which corresponds to the difference " $b-a$ ") is shown. Three of these pellets were surface ( $a = 0$ ) and two were subsurface ( $a > 0$ ) pellets. The surface pellet with a 3-mm active layer thickness had a catalytic zone with 6.8% silver as compared to 33.8% silver when the active layer was only 0.45 mm thick. From Figure 6, it is evident that when the silver is concentrated in thinner regions closer to the top surface (in other words, going from uniform to thin egg-shell pellets), the pellet performance improves: for the same conversion, selectivity and yield increase. On the other hand, when the silver is concentrated in thinner regions *inside* the pellet (in other words, moving from uniform to thin egg-white pellets), selectivity drops dramatically. These results verify that the *appropriate* Dirac distribution gives better performance than more uniform distributions. Note that the pellet with an inner Dirac distribution ( $a = 1.3 / b = 1.7$ ) shows worse performance than the two more uniform distributions ( $a = 0 / b = 3$  and  $a = 0.6 / b = 2.4$ ) centered at the same location ( $(a + b)/2$ ), which occurs because this is not the appropriate Dirac location.

## Concluding Remarks

A new single-pellet reactor design has been adopted in this study, which permits to investigate expeditiously the effect of the active layer location on the performance of silver catalyst for the ethylene epoxidation reaction network. The experimental results clearly demonstrate that the location of the catalytically active layer has a significant impact on catalyst performance.

The behavior of catalyst pellets, when the diffusional resistance is increased systematically, is altered as expected; the reaction rates decrease due to decreased reactant concentration at the location of the active layer. In certain cases, temperature gradients, both external and intraphase, become important as well. From the results obtained, it is evident that under the conditions employed, when either the selectivity or the yield to ethylene oxide is to be optimized, the optimal catalyst pellet is the one that has the thinnest active layer located at the external surface of the pellet. However, for sufficiently low temperatures and high inlet ethylene concentrations, it was found that the ethylene consumption and carbon dioxide production are higher in subsurface catalysts as compared to the surface one. These findings are in qualitative agreement with theoretical studies of ethylene epoxidation on Dirac-type catalysts. A quantitative comparison of experimental results with theoretical predictions is under way and will be reported in the future.

## Acknowledgment

We are grateful to Union Carbide Chemicals and Plastics Company for financial support of this work. We also thank Dr. Madan M. Bhasin for helpful discussions.

## Literature Cited

- Chemburkar, R. M., "Optimal Catalyst Activity Profiles in Pellets: Single Pellet Theory and Experiments," PhD Thesis, Univ. of Notre Dame (1987).
- Chemburkar, R. M., M. Morbidelli, and A. Varma, "Optimal Catalyst Activity Profiles in Pellets: VII. The Case of Arbitrary Reaction Kinetics with Finite External Heat and Mass Transport Resistances," *Chem. Eng. Sci.*, **42**, 2621 (1987).
- Czanderna, A. W., "The Adsorption of Oxygen on Silver," *J. Phys. Chem.*, **68**, 2765 (1964).
- Dougherty, R. C., and X. E. Verykios, "Nonuniformly Activated Catalysts," *Cat. Rev. Sci. Eng.*, **29**, 101 (1987).
- Kasaoka, S., and Y. Sakata, "Effectiveness Factors for Nonuniform Catalyst Pellets," *J. Chem. Eng. Japan*, **1**, 138 (1968).
- Klugherz, P. D., and P. Harriott, "Kinetics of Ethylene Oxidation on a Supported Silver Catalyst," *AIChE J.*, **17**, 856 (1971).
- Lee, C. K., and A. Varma, "An Isothermal Fixed-Bed Reactor with

- Nonuniformly Active Catalysts: Experiments and Theory," *Chem. Eng. Sci.*, **43**, 1995 (1988).
- Lee, J. K., X. E. Verykios, and R. Pitchai, "Support Participation in Chemistry of Ethylene Oxidation on Silver Catalysts," *Appl. Catal.*, **44**, 223 (1988).
- Masi, M., M. Sangalli, S. Carra, G. Cao, and M. Morbidelli, "Kinetics of Ethylene Hydrogenation on Supported Platinum. Analysis of Multiplicity and Nonuniformly Active Catalyst Particle Behavior," *Chem. Eng. Sci.*, **43**, 1849 (1988).
- Michalko, E., "Preparation of Catalyst for the Treatment of Combustible Waste Products," U.S. Patent 3,259,589 (July 5, 1966).
- Minhas, S., and J. J. Carberry, "On the Merits of Partially Impregnated Catalysts," *J. Catal.*, **14**, 270 (1969).
- Morbidelli, M., A. Servida, S. Carra, and A. Varma, "Optimal Catalyst Activity Profiles in Pellets: 3. The Nonisothermal Case with Negligible External Transport Limitations," *Ind. Eng. Chem. Fundam.*, **24**, 116 (1985).
- Morbidelli, M., A. Servida, R. Paludetto, and S. Carra, "Optimal Catalyst Design for Ethylene Oxide Synthesis," *J. Catal.*, **87**, 116 (1984).
- Morbidelli, M., A. Servida, and A. Varma, "Optimal Catalyst Activity Profiles in Pellets 1. The Case of Negligible External Mass Transfer Resistance," *Ind. Eng. Chem. Fundam.*, **21**, 278 (1982).
- Morbidelli, M., and A. Varma, "Optimal Catalyst Activity Profiles in Pellets: 2. The Influence of External Mass Transfer Resistance," *Ind. Eng. Chem. Fundam.*, **21**, 284 (1982).
- Pavlou, S., and C. G. Vayenas, "Optimal Catalyst Activity Distribution in Pellets for Selectivity Maximization in Triangular Nonisothermal Reaction Systems: Application to Cases of Light Olefin Epoxidation," *J. Catal.*, **122**, 389 (1990).
- Roth, J. F., and T. E. Reichard, "Determination and Effect of Platinum Concentration Profiles in Supported Catalysts," *J. Res. Inst. Catalysis, Hokkaido Univ.*, **20**, 85 (1972).
- Satterfield, C. N., *Heterogeneous Catalysis in Practice*, McGraw-Hill, New York (1980).
- Shadman-Yazdi, F., and E. E. Petersen, "Changing Catalyst Performance by Varying the Distribution of Active Catalyst within Porous Supports," *Chem. Eng. Sci.*, **27**, 227 (1972).
- Van Santen, R. A., and H. P. C. E. Kuipers, "The Mechanism of Ethylene Epoxidation," *Adv. Catal.*, **35**, 265 (1987).
- Vayenas, C. G., and S. Pavlou, "Optimal Catalyst Activity Distribution and Generalized Effectiveness Factors in Pellets: Single Reactions with Arbitrary Kinetics," *Chem. Eng. Sci.*, **42**, 2633 (1987).
- Vayenas, C. G., and S. Pavlou, "Optimal Catalyst Distribution for Selectivity Maximization in Nonisothermal Pellets: The Case of Parallel Reactions," *Chem. Eng. Sci.*, **43**, 2729 (1988).
- Wu, H., A. Brunovska, M. Morbidelli, and A. Varma, "Optimal Catalyst Activity Profiles in Pellets: VIII. General Nonisothermal Reacting Systems with Arbitrary Kinetics," *Chem. Eng. Sci.*, **45**, 1855 (1990a).
- Wu, H., Q. Yuan, and B. Zhu, "An Experimental Investigation of Optimal Active Catalyst Distribution in Nonisothermal Pellets," *Ind. Eng. Chem. Res.*, **27**, 1169 (1988).
- Wu, H., Q. Yuan, and B. Zhu, "An Experimental Study of Optimal Active Catalyst Distribution in Pellets for Maximum Selectivity," *Ind. Eng. Chem. Res.*, **29**, 1771 (1990b).

Manuscript received Sept. 6, 1991, and revision received Dec. 27, 1991.